Journal of the Optical Society of America B
OPTICAL PHYSICS

Scheme for sub-shot-noise transmission measurement using a time-multiplexed single-photon source

AGUSTINA G. MAGNONI,[1,2,*] LAURA T. KNOLL,[1,3] AND MIGUEL A. LAROTONDA[1,2,4]

[1]Laboratorio de Óptica Cuántica, DEILAP, UNIDEF (CITEDEF-CONICET), Buenos Aires, Argentina
[2]Departamento de Física, Facultad de Ciencias Exactas y Naturales, UBA, Ciudad de Buenos Aires, Argentina
[3]INRIM Istituto Nazionale di Ricerca Metrologica, Turin, Italy
[4]e-mail: mlarotonda@citedef.gob.ar
*Corresponding author: amagnoni@citedef.gob.ar

Received 16 April 2021; revised 8 July 2021; accepted 12 July 2021; posted 15 July 2021 (Doc. ID 428105); published 6 August 2021

Sub-shot-noise performance in transmission measurements can be achieved in optical quantum metrology owing to significantly lower uncertainty in light intensity of quantum beams compared to their classical counterparts. In this work, we simulate the outcome of an experiment that uses a multiplexed single-photon source, considering several types of experimental losses, where we show that the sub-Poissonian statistics of the output is key for achieving sub-shot-noise performance. We compare the numerical results with the *shot-noise limit* attained using coherent sources and the quantum limit, obtained with an ideal photon-number Fock state. We also investigate conditions in which threshold detectors can be used, as well as the effect of input light fluctuations. Our results show that sub-shot-noise performance can be achieved with improvement factors ranging from 1.5 to 2, even without using number-resolving detectors.

https://doi.org/10.1364/JOSAB.428105

1. INTRODUCTION

The field of quantum metrology and its applications in biological sciences [1–5] is a hot research topic. In particular, much attention has been paid to the utilization of quantum light as a resource for surpassing the classical limit of precision per unit intensity [6,7]. The ability to obtain a light source that operates below the shot-noise limit allows for performance improvement of tasks such as imaging of photo-reactive biological samples [8], high-precision optical activity measurements in chiral media [9], and high-sensitivity single biomolecule detection and tracking [10], among others.

This work is devoted to studying the behavior of a multiplexed single-photon source (an engineered light source that emits non-classical light states) [11] in the task of measuring the transmittance of a sample, to obtain an enhancement on the precision when compared to a measurement using classical light. Generally, the lower the intrinsic uncertainty in the intensity of the incident light, the more precise the result will be. The use of low-intensity light sources with sub-Poissonian statistics for absorption and transmission measurements is a promising technique for the study of fragile biological samples and ultrasensitive materials, since experiments can be performed with minimum disturbance [10,12,13].

The uncertainty of such measurement is given by the combination of random fluctuations, inherent in the optical probe beam, and the stochastic nature of the interaction between light and matter within the sampled object. By modeling two kinds of light sources, coherent states and Fock or number states, different precision limits can be obtained. In the former case, using a light source with Poissonian photon statistics to measure the transmittance of an object leads to a precision in the measurement bounded by the *shot-noise limit* (SNL): this is the best performance obtainable with classical light. Instead, the eventual use of an ideal antibunched light source such as a Fock state photon source gives the *ultimate quantum limit* (UQL) for the measurement precision, due to the deterministic nature of the photon number emission. This limit corresponds to the best quantum scenario. A large n-photon number Fock state source, however, is not an available resource yet. The challenge is therefore to obtain an engineered light source with intensity fluctuations below the Poissonian limit and to combine it with an adequate choice of an estimator, to obtain a measurement scheme that outperforms the classical one.

Real-world single-photon sources are an interesting option since an ideal N-photon Fock state as input achieves the same precision as an ideal single-photon input and N repetitions. High photon-number Fock states are not experimentally achievable nowadays, but a great deal of research is currently in progress to obtain devices that deliver light pulses carrying a single photon in well-defined spatio-temporal and polarization modes. Different approaches rely on either the use of

single-emitter sources, or some kind of multiplexing of one or several heralded photon pair sources based on the spontaneous parametric down conversion (SPDC). Single-emitter sources include devices based on fluorescence from atoms, ions, or molecules [14–17] and on different types of "artificial atoms." The single-photon emission from nitrogen-vacancy centers has been extensively reviewed in [18]. It has been known that quantum dots emit single photons since the end of the last century [19–23]. By coupling the quantum dots with electrically controlled cavities in deterministically fabricated devices, an enhancement on brightness and purity of these kinds of sources has been obtained, reaching indistinguishabilities above 99% and photon extraction efficiencies on the order of 66% [24,25]. Recently, the effect of imperfections and unwanted multi-photon components of such sources on the quality of the source has been studied both theoretically and experimentally [26].

Another approach to single-photon sources is based on nonlinear processes such as SPDC or four-wave mixing, where a pair of photons is produced after the interaction of one or two pump photons with a nonlinear material. One of the output photons is sent to a detector, which heralds with high probability the presence of the other photon, provided the two downconverted modes are non-degenerated in some degree of freedom. State-of-the-art implementations involve integrated optics devices and heralding efficiencies exceeding 50% [27,28] and even reaching 90% [29]. The heralding process removes the zero-photon component of the heralded field, but there is still a non-negligible probability of generating more than one pair, that scales with the pump intensity. Moreover, since these processes are probabilistic, there is a trade-off between the probability of generating a photon and the fidelity of the output to a single-photon state. By spatially multiplexing several heralded sources [30–36], temporally multiplexing a single source [37–45], or even combining temporal and spatial multiplexing [46], the source brightness can be (ideally) arbitrarily increased, depending on the size of the multiplexing network and its overall throughput. A comprehensive and updated review on such sources can be found in [11].

Meanwhile, transmission/absorption measurements have been widely studied recently. There are several different approaches to achieving the highest possible precision, which rely on different estimators and light sources, with and without spatial resolution. Schemes for estimating the transmission of a sample generally consist in measuring the intensity attenuation of a light beam that propagates through it, which can be done using a single light beam as the source (direct measurement), splitting the beam and using the tap to normalize the measurements and remove *excess noise* or avoid possible power drifts (differential measurement), or with twin-beam correlated sources. Twin-beams and difference-based estimators have been used for spatially resolved implementations [47], including the realization of the first sub-shot-noise wide-field microscope in 2017 [48]. The performance of this estimator depends on the spatial resolution and reaches out a factor of improvement in precision over the SNL of approximately 1.30. Estimators based on the ratio of two correlated beams have been first proposed in [49], and its recent experimental implementations use heralded single-photon sources and achieve a maximum improvement factor of 1.79 [50,51]. Another estimator based on the ratio of two signals but with some optimizations is presented in [52], reaching a maximum improvement factor of 1.46. Recently, a complete theoretical and experimental study of the performance of these different estimators was presented [53]. In these works, the reported improvement factors were obtained for transmissions 0.9 or higher.

In this work, we propose the use of a specific engineered single-photon-pulsed source [40,54] that relies on the correlations present in a photon pair SPDC source and on a binary-length division time-multiplexing network as the input of a direct-type transmission measurement. We compare its performance both with a weak coherent pulse source with Poissonian statistics (a "classical" experiment) and an ideal "photon gun," that is, a deterministic source that emits a single photon per pulse. The results can be adapted in a straightforward manner to essentially any single-photon source with known probability distribution for the emission. The advantage of a pulsed scheme compared with a heralded photon source is the fact that it easily allows for a minimum exposure of the sample to the probe beam by means of gating, while the stochastic nature of an heralded source requires some kind of active feed forward to reduce the illumination level or even to obtain a quantum advantage [49,50].

Another issue to consider to maximize measurement precision is the performance of the detection devices. Photon number-resolving (NR) detectors are the ultimate refinement for intensity detection and constitute the most sophisticated measurement devices for quantum optics. Different technological approaches are currently employed to obtain high-efficiency detectors with photon number resolution, such as arrays of multiplexed standard detectors [55,56], transition edge sensors [57–59], superconducting nanowire photon detectors (SNPD) [60–62], and even coupled charged devices with floating-gate amplifiers [63]. However, photon-counting detectors with low dark counts and mid-to-high efficiency such as avalanche photodiodes unable to resolve the number of detected photons (threshold detectors), are quite widespread, and their use is very common in research and metrology laboratories. We therefore study the behavior of the proposed setup under two different detection schemes: number resolving and threshold detectors.

This paper is organized as follows: in Section 2, we briefly review the main features of the proposed single-photon source. Section 3 is devoted to the discussion on the different transmission estimators used under the aforementioned detection conditions, and the discussion on the expected advantage that can be obtained with the single-photon source. In Section 4, we analyze the effect of fluctuations on the transmission estimation when the sources are fed with an optical pump governed by super-Poissonian photon statistics. Final remarks and comments regarding the perspective for the use of single-photon sources to obtain quantum advantage on transmission measurements are pointed out in Section 5.

2. TIME-MULTIPLEXED SINGLE-PHOTON SOURCE

The sub-Poissonian light source model studied here is a binary-time-multiplexed single-photon (BinMux-SP) source.

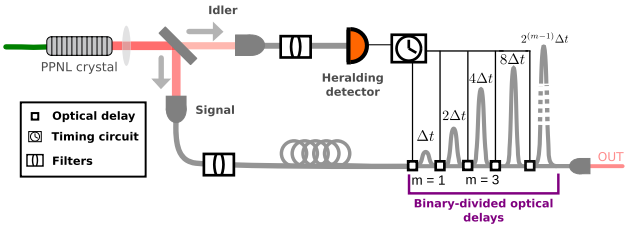

Fig. 1. Binary-time-multiplexed single-photon (BinMux-SP) source consists of a collinear, non-degenerate photon-pair generation stage, and a time-multiplexing stage that raises the single-photon probability and synchronizes the output photon to an external clock signal based on the timing of the herald photon detection. The latter stage is based on an array of several fiber optic fixed-length paths, each one imposing a different temporal delay to the signal photon.

This device is based on photon pairs (named signal and idler) obtained from an SPDC source with output mean μ, and a network of fiber optic components that conform the time-multiplexing stage (Fig. 1). This array has several possible fiber paths with different lengths that consequently impose different temporal delays to the signal photon. Which-path decision is made by a timing circuit, based on the information given by the detection of the idler photon. Given the external clock signal with period T, the time-multiplexing stage locates the signal photon (within a fixed short temporal window Δt) and re-routes it to the output, synchronized to the clock tick. Such scheme efficiently raises the single-photon probability and synchronizes the pulsed output state to an external clock signal.

The time-multiplexing network is binary divided with m possible delay stages, each one with a duration of $(2^{(i-1)}\Delta t)$, $i \in \{1, \cdots, m\}$. Active switching of this stages allows for compensation of a temporal mismatch (between the photon and the clock) up to $\mathcal{T} = (2^m - 1)\Delta t$. A detailed description of the source can be found in [40]. The probability mass function of emitting i photons of this source, $P_b^{(m)}(i)$, assuming no dark counts at the heralding detector was introduced and discussed in [54]:

$$P_b^{(m)}(i) = \sum_{n=i}^{\infty} \left[(1 - P(0, 2^m \mu e_h)) \frac{P(n, \mu)(1 - (1 - e_h)^n)}{\sum_j P(j, \mu)(1 - (1 - e_h)^j)} + P(0, 2^m \mu e_h) \frac{P(n, \mu)(1 - e_h)^n}{\sum_j P(j, \mu)(1 - e_h)^j} \right] \times \binom{n}{i} (e_s^{\text{tot}})^i (1 - e_s^{\text{tot}})^{n-i}. \tag{1}$$

$P_b^{(m)}(i)$ depends on the following experimentally accessible parameters: μ, the initial photon–pair rate per detection window Δt; m, the number of correcting stages; e_h, the overall efficiency of the heralding branch; $e_s^{\text{tot}} = e_s \times (e_{sw})^{m+1}$, the overall transmission of the signal (or heralded) branch (with e_{sw} each switch's transmission). $P(j, \alpha)$ is the Poisson probability of obtaining j photons on a trial with a mean photon number α. The last term of the product on each element of the sum is the binomial distribution $B(x|p, n) \equiv \binom{n}{x} p^x (1 - p)^{n-x}$ that considers the unavoidable loss on the switching network. This term depends on the amount of delay stages used and takes into account other possible general optical losses of the branch.

The shortest correcting time of the network was set to $\Delta t = 2$ ns, constrained by the coherence length of the photon pair and by the photo-detection jitter at the heralding side. The efficacy of the setup as a sub-Poissonian photon gun relies on the ability to obtain a high probability of detecting at least one photon during the total synchronization interval T—thus minimizing the zero-photon component of the distribution—together with a low probability of multi-photon occurrence within a single temporal window Δt. Optimum conditions for fixed number of delay stages (or *correction stages*) and loss can be obtained by adjusting the input mean photon pair number μ from the SPDC source. Throughout this paper, the other parameters have been set to $e_h = 0.8$ and $e_{sw} = 0.9$ (0.5 dB insertion loss).

3. TRANSMISSION ESTIMATORS

Following the strategy of using many single photons instead of a large-number Fock state as input, we study the performance of the BinMux-SP in a direct single beam transmission measurement scheme, like the one depicted in Fig. 2. We compare its performance by replacing the BinMux-SP with a source of weak coherent pulses and with a perfect single-photon source. We consider an optical loss of $e_s = 0.9$ for the coherent and BinMux-SP cases, which is included within the probability distributions, while we use a lossless channel for the Fock state source.

The performance of the different estimators $(\hat{T})$ of a given parameter (t) can be compared by computing their expected value E, and their mean squared error (MSE). These quantities depend on the random variable k that is being measured and its probability distribution $\mathcal{P}(k)$ [64,65]:

$$E(\hat{T}) = \sum_k \hat{T}(k)\mathcal{P}(k), \tag{2}$$

$$\text{MSE}(\hat{T}) = \sum_k [\hat{T}(k) - t]^2 \mathcal{P}(k), \tag{3}$$

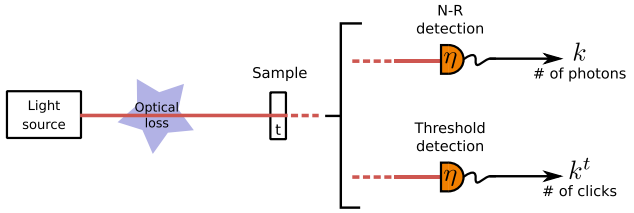

Fig. 2. General scheme for a direct transmission measurement: a light source sends a beam through the sample, and the transmitted light is detected afterwards. The detector efficiency is $\eta = 0.9$, and it may or may not have an NR capacity. The measured random variables are k, the number of detected photons in the former case, and k^t, the number of detector clicks in the latter. This procedure is repeated ν rounds. Lenses and other optical elements can impose an additional loss between the source and the sample. For the non-ideal sources studied, we consider an optical loss of 0.9, while we do not consider any optical loss for the ideal Fock-state photon source.

for discrete probability distributions. Throughout this work, k represents the number of detected events on each experiment. The benefit of using the MSE over the variance ($\mathrm{Var}(\hat{T}) = \sum_k [\hat{T}(k) - \mathrm{E}(\hat{T})]^2 \mathcal{P}(k)$), is that it considers both the precision and the accuracy of the estimator. These quantities enable us to simulate the performance of the estimators using the real value of the parameter.

In what follows we introduce transmission estimators both for NR and threshold detectors. The efficiency of both detectors is set to $\eta = 0.9$. Detector dark counts are not considered, since the pulsed characteristics of the sources allow for fast gating and dark count rates per pulse $<10^{-6}$ can be achieved with any state-of-the-art detection device.

Throughout the work, we assign the SNL performance to the coherent state photon source illuminating a translucent sample using a NR detector, and the UQL performance with the single-photon Fock state, which given its nature, does not change with the choice of the detector.

A. Estimators for NR Detectors

When using NR detectors, the measured random variable k is the detected number of photons. For the three different sources considered in this work, the emission probability distribution of i photons is Poissonian in the coherent case $P(i, \alpha)$, sub-Poissonian in BinMux-SP with m delay stages $P_b^{(m)}(i)$ [54], and a perfect number state—with null variance—in the single-photon Fock case. The inefficiency of the detection process combines the emission distribution with an additional binomial distribution in each case to describe the statistics of the random variable k.

The general form of the transmission estimators for each case are

$$\text{Coherent}: \quad \hat{T}_c^{nr}(k_c) = \frac{k_c}{\eta * \langle n_c \rangle}, \tag{4}$$

$$\text{BinMux}-\text{SP}: \quad \hat{T}_b^{nr}(k_b) = \frac{k_b}{\eta * \langle n_b \rangle}, \tag{5}$$

$$\text{Fock}: \quad \hat{T}_f^{nr}(k_f) = \frac{k_f}{\eta N_{in}}. \tag{6}$$

The measured number of photons in the experiments with coherent BinMux-SP and Fock pulsed sources is k_c, k_b, and k_f, respectively; η is the detector efficiency (which is set to 0.9 throughout the simulations), $\langle n \rangle$ is the mean number of photons per pulse incident on the sample, and N_{in} is the eigenvalue of the photon number operator in the case of Fock states. In particular, we set $N_{in} = 1$ and $\alpha = \langle n_c \rangle = 1$, $\langle n_b \rangle = 1$ for Subsections 3.A and 3.B. Since the relative error is high in such a low-intensity regime, we also considered $\nu = 200$ as the number of repetitions of the experiment for all simulations presented in these subsections, to reduce the uncertainty of the measurement. The performance of these estimators was studied using their definitions, Eqs. (4)–(6), and the explicit expressions of the probability distributions of the random variables k to compute the mean and the MSE using Eqs. (2) and (3).

The first important property of these estimators is that they are accurate (or unbiased) for all three sources: the expected value is equal to the transmission parameter, which also means that the MSE is equal to the variance. To study the improvement factor, we computed the ratio between the MSE of the coherent source (what we call the SNL) to the MSE of each source [Fig. 3(A)]. For the BinMux-SP, we studied the performance of a different number of correction stages m (Section 2). Analyzing the ratios enables for a quick check of the quantum advantage (ratio >1) and also independence from the number of repetitions (ν). Repetitions only raise the precision equally for all sources (in the case of unbiased estimators), reducing the variance by a factor ν. The MSE as a function of the transmission alone can be observed in Fig. 3(B).

It is clear that for the case of the BinMux-SP source, there is an advantage over the shot-noise limit for the complete transmission range. The enhancement on the source statistics obtained by increasing the number of correcting stages is eventually compensated by the loss introduced at each switching element. The choice of experimental parameters for this simulation implies that the maximum ratio is obtained for $m = 2$. For the selected correcting time $\Delta t = 2$ ns, this corresponds to a source output repetition rate of 250 MHz. Regarding the absolute value of the MSE (or variance, in this case), it can be further reduced by increasing the number of repetitions ν. It is important to note that these estimators are close to the optimum for the probability distribution of the BinMux-SP source: the variance approaches the limit imposed by the Cramér–Rao bound, which sets a lower bound on the variance of unbiased estimators of a given parameter, for a particular experiment [66].

B. Threshold Detectors

Even though there has been substantial attention and significant progress in the development of photon NR detectors [61], they are still expensive and resource-demanding pieces of equipment. In contrast, standard photon-counting devices with binary output (detection-no detection) are quite common in quantum optics and metrology laboratories. It is therefore interesting to study the changes introduced by replacing the NR detectors with threshold detectors, considering the high efficiencies achieved [67] and the low-intensity working scenario.

By replacing the NR detectors, the measured random variable changes from number of photons to *detector clicks*, each one of them triggered by the arrival of one or more photons. The previous estimators (4)–(6) can be adapted in a straightforward fashion: in this condition, k^t represents the total number of clicks after the sample and $\langle n^t \rangle$ the mean number of clicks without sample, in ν repetitions of the experiment:

$$\text{Coherent}: \quad \hat{T}_c^{t}(k_c^t) = \frac{k_c^t}{\langle n_c^t \rangle}, \tag{7}$$

$$\text{BinMux}-\text{SP}: \quad \hat{T}_b^{t}(k_b^t) = \frac{k_b^t}{\langle n_b^t \rangle}, \tag{8}$$

$$\text{Fock}: \quad \hat{T}_f^{t}(k_f^t) = \frac{k_f^t}{\eta N_{in}}. \tag{9}$$

The probability distributions of k^t are now binomials $B(k^t | p^{click}, \nu)$, with ν trials (number of repetitions), k^t successes, and a probability of success per trial p^{click}. This p^{click}

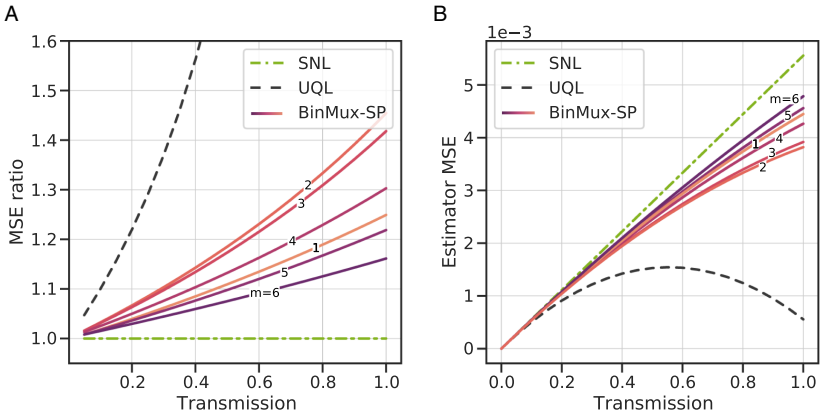

Fig. 3. (A) MSE ratio between the coherent source (SNL) and either the BinMux-SP (with one to six correction stages m) or the single-photon Fock state (UQL). (B) MSE for the SNL, the BinMux-SP source, and the UQL.

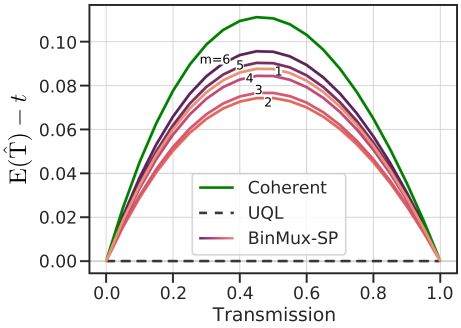

Fig. 4. Difference between the mean of the estimator and the transmission as a function of the latter for the three sources (coherent, BinMux-SP, and single-photon Fock states [UQL]) using threshold detectors.

success probability corresponds to the probability of having a click in the detector per trial, and it can be calculated for each case as follows:

$$\text{Coherent}: \quad p_c^{\text{click}} = \sum_{i\geq 1}[1 - B(0|t\eta, i)]P(i, \alpha), \tag{10}$$

$$\text{BinMux}-\text{SP}: \quad p_b^{\text{click}} = \sum_{i\geq 1}[1 - B(0|t\eta, i)]P_b^{(m)}(i), \tag{11}$$

$$\text{Fock}: \quad p_f^{\text{click}} = t\eta. \tag{12}$$

These consider i photons emitted from each respective source (with Poissonian probability $P(i, \alpha)$ for the coherent case, $P_b^{(m)}(i)$ for the BinMux source [54], and 1 for the Fock state) and at least one of them being detected, surviving both the sample and the detection efficiency. This survival is accounted for in the $\sum_{i\geq 1}[1 - B(0|t\eta, i)]$ terms for the first two sources and, more simply, with $t\eta$ in the Fock case.

Because of the nature of the detection process, an increase in the multi-photon emission probability of the source lowers the correlation between a single photon and a click.

As expected, these estimators are biased for the coherent and the BinMux-SP cases, and unbiased for the Fock states. This can be seen in Fig. 4, which shows the difference between the mean of the estimator and the true value of the transmission.

The sub-Poissonian statistics of the BinMux-SP source are responsible for the reduced bias in the estimators. This behavior is observable in the MSE ratios and in the MSE alone, as shown in Figs. 5(A) and 5(B), respectively. In this case, using the BinMux-SP source is favorable only for a limited range of transmissions close to the transparent $t = 1$ limit. However, in this region, the performance of the SNL can be significantly improved (in some cases with a ratio >2). Additionally, it is always a better alternative to the coherent source with a threshold detector. It is also worth noting that for high transmissions, an advantage over the SNL can be obtained by using a threshold detector with the coherent state. This is due to the variance-reduction effect of the binarization introduced by the threshold detection, which has only two possible outcomes: click or no-click [68].

However, unlike the case of unbiased estimators, it is not possible to arbitrarily reduce the MSE by increasing the number of repetitions ν. The MSE has a fundamental limit, given by the inaccuracy of the estimators: it can not be smaller than the squared of the difference between the mean and the parameter (Fig. 4). However, since the estimator is not biased for $t = 0$ and $t = 1$, a good performance can always be obtained for high transmission values.

Even though a fair comparison with the single-photon Fock state would correspond to input mean photon numbers $\langle n_c\rangle = \langle n_b\rangle = 1$, and given that the bias in the threshold estimators is mainly due to the multi-photon components of the statistics, it would be interesting to explore the performance of the estimators for lower intensity values. In the next section, we study how these results are modified for different input intensities.

C. Lower Light Intensity Regimes

Lowering the mean number of photons per pulse to reduce the amount of multi-photon emission is a common strategy when using a weak coherent pulse source. The sub-Poissonian nature of the BinMux-SP statistics also guarantees a more efficient response to this action, showing an improved reduction on the multi-photon pulses compared to that of the coherent source.

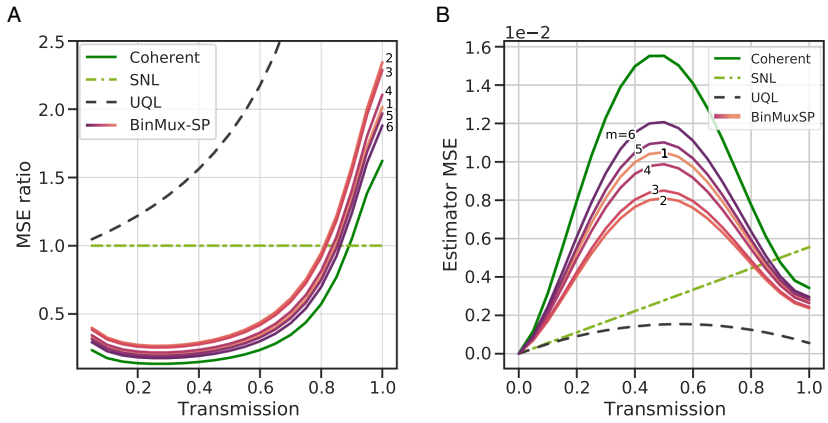

Fig. 5. (A) MSE ratios for the threshold detection case. One of the reference curves (from which the ratios are computed) is again the one obtained using a coherent source with NR detectors (SNL). The other reference is the MSE ratio for a single-photon Fock state (UQL). (B) MSE for the same sources, together with the SNL reference (light-green curve) for direct comparison.

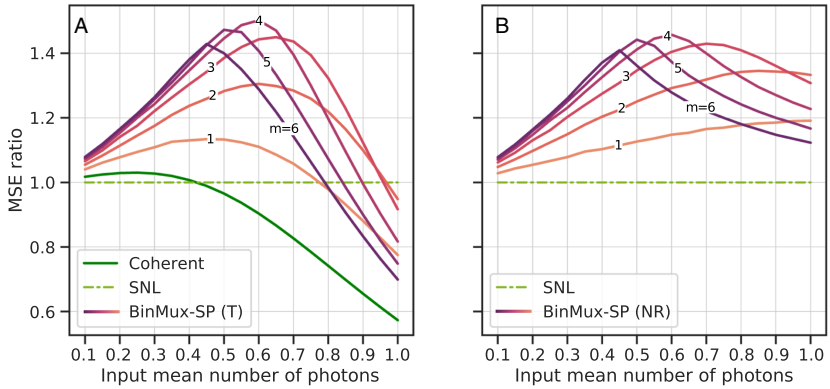

Fig. 6. MSE ratio for a sample transmission $t = 0.8$ as a function of the input mean number of photons for (A) the threshold estimators and (B) the NR estimators, when $\nu = 200$. The vertical axis is shared for both plots.

Figure 6 shows results for a sample transmission $t = 0.8$. Although for a unity input mean photon number, the estimators with threshold detectors do not present any enhancement over the SNL, an advantage can be still obtained for lower intensities. Indeed, MSE ratios of ∼1.5 can be achieved, which is very similar to the best performance available with NR detectors. The reduced intensity condition at the output of the source also enhances the effect of the switching network, and the net result is that the optimum condition is obtained for a higher number of compensating stages m. It is also interesting to note that, for this transmission range and number of repetitions, the coherent source with threshold detection barely outperforms the SNL between 0 and 0.4 mean photon number.

The overall behavior is representative of the source performance for mid-range transmissions. This analysis enables a rapid visualization for selecting the most convenient combination of number of correcting stages m on the BinMux-SP source and input mean photon number, for a given value of the transmission.

Given that the estimators for threshold detectors are indeed biased, the improvement of their performance is therefore limited by the asymptotic limit imposed by their inaccuracy, while the NR detector estimators only get more precise. In Fig. 7, we present the asymptotic minimum relative MSE, achievable per transmission value, for three representative values of input mean photon number, both for the coherent and the BinMux-SP sources.

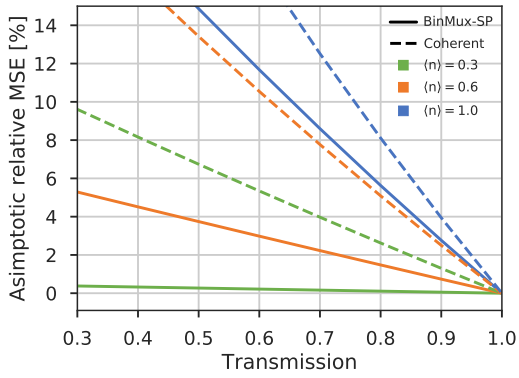

Fig. 7. Asymptotic minimum relative MSE (%) achievable as a function of the transmission. These values correspond to a very large number of repetitions ν, and they are thus caused by the inaccuracy of the estimators. Solid line corresponds to the BinMux-SP source and the dashed line to the coherent source.

These values of MSE can be accessed by performing a very large number of repetitions; in this situation the inaccuracy

eventually dominates over the precision. As expected, the MSE% is greatly influenced by the intensity used. The enhancement obtained with the use of the BinMux-SP source over a coherent source is present for all transmissions in all three values of $\langle n \rangle$, and for mid-range transmission values, a threefold increase can be obtained.

4. EFFECT OF FLUCTUATIONS IN THE INPUT LIGHT SOURCE

Both the BinMux-SP and the coherent sources must be fed with a light source governed by Poissonian statistics; in the coherent case, it is the source itself, whereas the BinMux-SP is based on a parametric fluorescence photon pair source, which for practical purposes, shows Poissonian statistics on the pair emission. A technique to minimize excess noise produced by super-Poissonian light sources is to monitor the photon rate of a portion of the beam before interacting with the sample, to compensate for any drift. Such *differential measurement* may not always be possible to implement, and therefore, it is interesting to study the robustness of the method against excess fluctuations in a *direct transmission measurement* scheme, considering the mean photon number of the coherent source α, and the mean photon pair rate that feeds the multiplexed source μ as a random variable with Gaussian statistics. Their respective standard deviations are $\sigma_c = a\alpha$ and $\sigma_b = a\mu$, $a \in \{0, \cdots, 0.6\}$. For the following discussion, the mean value of this distribution is chosen to be $\alpha = \langle n_c \rangle = 0.5, \langle n_b \rangle = 0.5$.

The estimator MSE for a transmission $t = 0.8$ as a function of the size of the fluctuations (i.e., a in %) for both types of detectors is shown in Fig. 8, for two representative amounts of correction stages m for the BinMux-SP.

Since the reference beam in this direct type of measurements is computed without fluctuations (or considering a significant amount of integration time that ensures compensation), the larger the fluctuations, the greater the MSE observed; this is primarily caused by the bias introduced in the measurement. For the coherent source in the NR case, the MSE at maximum fluctuation is 3.4 times its original value, while for $m = 5$ BinMux-SP, it is 2.1, in agreement with the results shown in Fig. 6(A). This effect is slightly reduced when using threshold detectors due to the variance reduction introduced (referred to in Section 3.B).

At the same time, the width of the 68% confidence interval is larger and more dependent on the fluctuations for the coherent source than for the BinMux-SP source, for both types of detectors.

These results show that the effect of raising the single-photon probability introduced by the time-multiplexing stage in the BinMux-SP source also guarantees a more robust output flux against fluctuations of the pump-power intensity. This is mainly because less intensity is required at the input to achieve a certain mean number of photons at the output, an effect that increases with an increasing number of correcting stages. Taking into account that perfect Poissonian coherent sources (that would require laser sources with perfectly stable output) are not easily attainable experimentally, this feature of the BinMux-SP source is also of great importance.

5. FINAL REMARKS AND DISCUSSION

In this work, we studied the use of a time-multiplexed single-photon source (BinMux-SP) as an input for transmission/absorption measurements, and we investigated its performance in obtaining a quantum enhancement in such tasks. Perfect number Fock states can achieve the ultimate quantum limit in this type of measurements, but represent a technological challenge, particularly for large number states. The proposed strategy is to approach the ν number perfect Fock state performance using single-photon states generated from the BinMux-SP source as input and performing ν repetitions.

We investigate a direct measurement scheme, comparing the number of photons detected with and without sample. Due to the single-photon nature of the sources, we have built estimators for both NR and threshold detectors. Working with threshold detectors and achieving sub-shot-noise performance is a desirable goal due to their widespread use in quantum optics and metrology laboratories.

In terms of accuracy, NR estimators are unbiased, as opposed to threshold estimators: while the precision can be arbitrarily reduced by the number of repetitions in the NR case, a fundamental limit exists in the threshold case. Nonetheless, the bias is non-trivially reduced to zero for $t = 1$, indicating that an

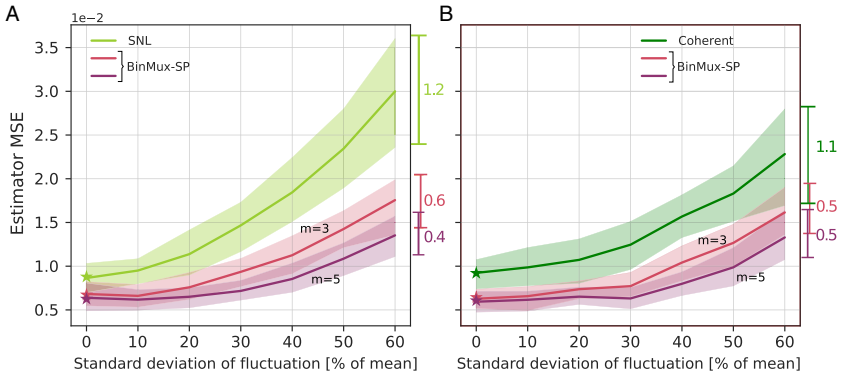

Fig. 8. Estimator MSE for (A) the NR detectors and (B) the threshold detectors, as a function of the amount of fluctuation present in the incident light (the standard deviation as a percentage of the mean). The solid line corresponds to the mean MSE (obtained over 50 rounds), whereas the shaded region shows the 68% confidence interval. The behavior with $m = 3$ and $m = 5$ correcting stages is shown. Figures at the right of each plot correspond to the confidence interval for the maximum fluctuation considered.

acceptable performance can still be obtained for low absorption samples. Explicitly, for a transmission $t = 0.98$, an enhancement factor of 2.2 over the SNL can be achieved with $\nu = 200$ repetitions, and $\langle n_b \rangle = 1$ using the BinMux-SP source with threshold detectors. This measurement implies a relative MSE of 5%.

For increased absorption, it is convenient to work at even lower mean photon numbers, to reduce the effect of the bias. Halving the photon flux, an enhancement factor of 1.4 can be achieved with $\nu = 2000$ repetitions on samples with a 20% absorption.

In the NR case, for a transmissions of $t = 0.98$ and $t = 0.8$, maximum enhancement factors of 1.6 and 1.45 can be achieved respectively, using $\langle n_b \rangle = 0.6$. The relative MSE can be arbitrarily reduced, due to the zero bias of the estimators.

A key issue is that the pulsed source output has sub-Poissonian statistics. This means that sub-shot noise uncertainties can be obtained for illumination levels as low as a single photon per detection window. Dynamic biological measurements require low light levels to avoid sample damage. With this constraint on optical power, quantum noise fundamentally limits the measurement sensitivity, and this limit can only be surpassed by extracting more information per photon. The fact that the source is pulsed allows for accurate and fast triggering, limiting the sample exposure only to pre-selected photons. Even though repetitive sampling using a strong classical source may lead to a high precision measurement, fragile samples might not be studied in this way. We have also shown that the performance of a temporally multiplexed single-photon source is less influenced by super-Poissonian fluctuations than that of a coherent source with excess noise. This is an interesting result for real-life imperfect experimental implementations.

The results presented in this work encourage the use of single-photon sources as suitable input beams for transmission estimation, while achieving a large quantum enhancement. Equivalent results can be obtained for any multiplexed source with known emission probability distribution and sub-Poissonian statistics. Particularly, this study on the performance of the BinMux-SP source taking into account several experimental imperfections shows that single-photon sources built from SPDC and time-multiplexing strategies represent a valid, cost-effective and room temperature alternative to other single-photon sources.

Funding. Ministerio de Defensa, Argentina (PIDDEF 02/16); Consejo Nacional de Investigaciones Científicas y Técnicas (PIP CONICET 0648-2014).

Disclosures. The authors declare no conflicts of interest.

Data Availability. Data underlying the results presented in this paper are not publicly available at this time but may be obtained from the authors upon reasonable request.

REFERENCES

1. V. Giovannetti, S. Lloyd, and L. Maccone, "Advances in quantum metrology," Nat. Photonics **5**, 222–229 (2011).
2. M. A. Taylor and W. P. Bowen, "Quantum metrology and its application in biology," Phys. Rep. **615**, 1–59 (2016).
3. M. R. Wasielewski, M. D. Forbes, N. L. Frank, K. Kowalski, G. D. Scholes, J. Yuen-Zhou, M. A. Baldo, D. E. Freedman, R. H. Goldsmith, T. Goodson, III, M. L. Kirk, J. K. McCusker, J. P. Ogilvie, D. A. Shultz, S. Stoll, and K. B. Whaley, "Exploiting chemistry and molecular systems for quantum information science," Nat. Rev. Chem. **4**, 490–504 (2020).
4. O. S. Magaña-Loaiza and R. W. Boyd, "Quantum imaging and information," Rep. Prog. Phys. **82**, 124401 (2019).
5. S. Pang and A. N. Jordan, "Optimal adaptive control for quantum metrology with time-dependent hamiltonians," Nat. Commun. **8**, 14695 (2017).
6. I. R. Berchera and I. P. Degiovanni, "Quantum imaging with sub-poissonian light: challenges and perspectives in optical metrology," Metrologia **56**, 024001 (2019).
7. P.-A. Moreau, E. Toninelli, T. Gregory, and M. J. Padgett, "Imaging with quantum states of light," Nat. Rev. Phys. **1**, 367–380 (2019).
8. A. Meda, E. Losero, N. Samantaray, F. Scafirimuto, S. Pradyumna, A. Avella, I. Ruo-Berchera, and M. Genovese, "Photon-number correlation for quantum enhanced imaging and sensing," J. Opt. **19**, 094002 (2017).
9. S.-J. Yoon, J.-S. Lee, C. Rockstuhl, C. Lee, and K.-G. Lee, "Experimental quantum polarimetry using heralded single photons," Metrologia **57**, 045008 (2020).
10. N. Mauranyapin, L. Madsen, M. Taylor, M. Waleed, and W. Bowen, "Evanescent single-molecule biosensing with quantum-limited precision," Nat. Photonics **11**, 477–481 (2017).
11. E. Meyer-Scott, C. Silberhorn, and A. Migdall, "Single-photon sources: approaching the ideal through multiplexing," Rev. Sci. Instrum. **91**, 041101 (2020).
12. G. Zonios, A. Dimou, I. Bassukas, D. Galaris, A. Tsolakidis, and E. Kaxiras, "Melanin absorption spectroscopy: new method for non-invasive skin investigation and melanoma detection," J. Biomed. Opt. **13**, 014017 (2008).
13. M. T. Cone, J. D. Mason, E. Figueroa, B. H. Hokr, J. N. Bixler, C. C. Castellanos, G. D. Noojin, J. C. Wigle, B. A. Rockwell, V. V. Yakovlev, and E. S. Fry, "Measuring the absorption coefficient of biological materials using integrating cavity ring-down spectroscopy," Optica **2**, 162–168 (2015).
14. F. Diedrich and H. Walther, "Nonclassical radiation of a single stored ion," Phys. Rev. Lett. **58**, 203–206 (1987).
15. H. J. Kimble, M. Dagenais, and L. Mandel, "Photon antibunching in resonance fluorescence," Phys. Rev. Lett. **39**, 691–695 (1977).
16. L. Mandel, "Sub-poissonian photon statistics in resonance fluorescence," Opt. Lett. **4**, 205–207 (1979).
17. T. Basché, W. Moerner, M. Orrit, and H. Talon, "Photon antibunching in the fluorescence of a single dye molecule trapped in a solid," Phys. Rev. Lett. **69**, 1516–1519 (1992).
18. I. Aharonovich, D. Englund, and M. Toth, "Solid-state single-photon emitters," Nat. Photonics **10**, 631–641 (2016).
19. C. Couteau, S. Moehl, F. Tinjod, J. Gérard, K. Kheng, H. Mariette, J. Gaj, R. Romestain, and J. Poizat, "Correlated photon emission from a single II–VI quantum dot," Appl. Phys. Lett. **85**, 6251–6253 (2004).
20. M. J. Holmes, K. Choi, S. Kako, M. Arita, and Y. Arakawa, "Room-temperature triggered single photon emission from a III-nitride site-controlled nanowire quantum dot," Nano Lett. **14**, 982–986 (2014).
21. K. Sebald, P. Michler, T. Passow, D. Hommel, G. Bacher, and A. Forchel, "Single-photon emission of CdSe quantum dots at temperatures up to 200 K," Appl. Phys. Lett. **81**, 2920–2922 (2002).
22. D. Gammon, E. Snow, B. Shanabrook, D. Katzer, and D. Park, "Homogeneous linewidths in the optical spectrum of a single gallium arsenide quantum dot," Science **273**, 87–90 (1996).
23. P. Michler, A. Kiraz, C. Becher, W. Schoenfeld, P. Petroff, L. Zhang, E. Hu, and A. Imamoglu, "A quantum dot single-photon turnstile device," Science **290**, 2282–2285 (2000).
24. X. Ding, Y. He, Z.-C. Duan, N. Gregersen, M.-C. Chen, S. Unsleber, S. Maier, C. Schneider, M. Kamp, S. Höfling, C.-Y. Lu, and J.-W. Pan, "On-demand single photons with high extraction efficiency and near-unity indistinguishability from a resonantly driven quantum dot in a micropillar," Phys. Rev. Lett. **116**, 020401 (2016).
25. N. Somaschi, V. Giesz, L. De Santis, J. Loredo, M. P. Almeida, G. Hornecker, S. L. Portalupi, T. Grange, C. Antón, J. Demory, C. Gómez, I. Sagnes, N. D. Lanzillotti-Kimura, A. Lemaítre, A. Auffeves,

A. G. White, L. Lanco, and P. Senellart, "Near-optimal single-photon sources in the solid state," Nat. Photonics **10**, 340–345 (2016).
26. H. Ollivier, S. E. Thomas, S. C. Wein, I. M. de Buy Wenniger, N. Coste, J. C. Loredo, N. Somaschi, A. Harouri, A. Lemaitre, I. Sagnes, L. Lanco, C. Simon, C. Anton, O. Krebs, and P. Senellart, "Hong-Ou-Mandel interference with imperfect single photon sources," Phys. Rev. Lett. **126**, 063602 (2021).
27. M. Bock, A. Lenhard, C. Chunnilall, and C. Becher, "Highly efficient heralded single-photon source for telecom wavelengths based on a PPLN waveguide," Opt. Express **24**, 23992–24001 (2016).
28. N. Montaut, L. Sansoni, E. Meyer-Scott, R. Ricken, V. Quiring, H. Herrmann, and C. Silberhorn, "High-efficiency plug-and-play source of heralded single photons," Phys. Rev. Appl. **8**, 024021 (2017).
29. S. Paesani, M. Borghi, S. Signorini, A. Manos, L. Pavesi, and A. Laing, "Near-ideal spontaneous photon sources in silicon quantum photonics," Nat. Commun. **11**, 2505 (2020).
30. A. L. Migdall, D. Branning, and S. Castelletto, "Tailoring single-photon and multiphoton probabilities of a single-photon on-demand source," Phys. Rev. A **66**, 053805 (2002).
31. J. H. Shapiro and F. N. Wong, "On-demand single-photon generation using a modular array of parametric downconverters with electro-optic polarization controls," Opt. Lett. **32**, 2698–2700 (2007).
32. T. Jennewein, M. Barbieri, and A. G. White, "Single-photon device requirements for operating linear optics quantum computing outside the post-selection basis," J. Mod. Opt. **58**, 276–287 (2011).
33. X.-S. Ma, S. Zotter, J. Kofler, T. Jennewein, and A. Zeilinger, "Experimental generation of single photons via active multiplexing," Phys. Rev. A **83**, 043814 (2011).
34. A. Christ and C. Silberhorn, "Limits on the deterministic creation of pure single-photon states using parametric down-conversion," Phys. Rev. A **85**, 023829 (2012).
35. M. J. Collins, C. Xiong, I. H. Rey, T. D. Vo, J. He, S. Shahnia, C. Reardon, T. F. Krauss, M. Steel, A. S. Clark, and B. J. Eggleton, "Integrated spatial multiplexing of heralded single-photon sources," Nat. Commun. **4**, 2582 (2013).
36. L. Mazzarella, F. Ticozzi, A. V. Sergienko, G. Vallone, and P. Villoresi, "Asymmetric architecture for heralded single-photon sources," Phys. Rev. A **88**, 023848 (2013).
37. E. Jeffrey, N. A. Peters, and P. G. Kwiat, "Towards a periodic deterministic source of arbitrary single-photon states," New J. Phys. **6**, 100 (2004).
38. J. Mower and D. Englund, "Efficient generation of single and entangled photons on a silicon photonic integrated chip," Phys. Rev. A **84**, 052326 (2011).
39. B. L. Glebov, J. Fan, and A. Migdall, "Deterministic generation of single photons via multiplexing repetitive parametric downconversions," Appl. Phys. Lett. **103**, 031115 (2013).
40. C. T. Schmiegelow and M. A. Larotonda, "Multiplexing photons with a binary division strategy," Appl. Phys. B **116**, 447–454 (2014).
41. F. Kaneda, B. G. Christensen, J. J. Wong, H. S. Park, K. T. McCusker, and P. G. Kwiat, "Time-multiplexed heralded single-photon source," Optica **2**, 1010–1013 (2015).
42. G. J. Mendoza, R. Santagati, J. Munns, E. Hemsley, M. Piekarek, E. Martín-López, G. D. Marshall, D. Bonneau, M. G. Thompson, and J. L. O'Brien, "Active temporal and spatial multiplexing of photons," Optica **3**, 127–132 (2016).
43. P. P. Rohde, L. Helt, M. Steel, and A. Gilchrist, "Multiplexed single-photon-state preparation using a fiber-loop architecture," Phys. Rev. A **92**, 053829 (2015).
44. X. Zhang, Y. Lee, B. Bell, P. Leong, T. Rudolph, B. Eggleton, and C. Xiong, "Indistinguishable heralded single photon generation via relative temporal multiplexing of two sources," Opt. Express **25**, 26067–26075 (2017).
45. F. Kaneda and P. G. Kwiat, "High-efficiency single-photon generation via large-scale active time multiplexing," Sci. Adv. **5**, eaaw8586 (2019).
46. P. Adam, M. Mechler, I. Santa, and M. Koniorczyk, "Optimization of periodic single-photon sources," Phys. Rev. A **90**, 053834 (2014).
47. G. Brida, M. Genovese, and I. R. Berchera, "Experimental realization of sub-shot-noise quantum imaging," Nat. Photonics **4**, 227–230 (2010).
48. N. Samantaray, I. Ruo-Berchera, A. Meda, and M. Genovese, "Realization of the first sub-shot-noise wide field microscope," Light Sci. Appl. **6**, e17005 (2017).
49. E. Jakeman and J. Rarity, "The use of pair production processes to reduce quantum noise in transmission measurements," Opt. Commun. **59**, 219–223 (1986).
50. J. Sabines-Chesterking, R. Whittaker, S. Joshi, P. Birchall, P.-A. Moreau, A. McMillan, H. Cable, J. O'Brien, J. Rarity, and J. Matthews, "Sub-shot-noise transmission measurement enabled by active feed-forward of heralded single photons," Phys. Rev. Appl. **8**, 014016 (2017).
51. J. Sabines-Chesterking, A. McMillan, P. Moreau, S. Joshi, S. Knauer, E. Johnston, J. Rarity, and J. Matthews, "Twin-beam sub-shot-noise raster-scanning microscope," Opt. Express **27**, 30810–30818 (2019).
52. P.-A. Moreau, J. Sabines-Chesterking, R. Whittaker, S. K. Joshi, P. M. Birchall, A. McMillan, J. G. Rarity, and J. C. Matthews, "Demonstrating an absolute quantum advantage in direct absorption measurement," Sci. Rep. **7**, 6256 (2017).
53. E. Losero, I. Ruo-Berchera, A. Meda, A. Avella, and M. Genovese, "Unbiased estimation of an optical loss at the ultimate quantum limit with twin-beams," Sci. Rep. **8**, 7431 (2018).
54. A. G. Magnoni, I. H. L. Grande, L. T. Knoll, and M. A. Larotonda, "Performance of a temporally multiplexed single-photon source with imperfect devices," Quantum Inf. Process. **18**, 311 (2019).
55. D. Achilles, C. Silberhorn, C. Śliwa, K. Banaszek, and I. A. Walmsley, "Fiber-assisted detection with photon number resolution," Opt. Lett. **28**, 2387–2389 (2003).
56. M. Fitch, B. Jacobs, T. Pittman, and J. Franson, "Photon-number resolution using time-multiplexed single-photon detectors," Phys. Rev. A **68**, 043814 (2003).
57. A. E. Lita, A. J. Miller, and S. W. Nam, "Counting near-infrared single-photons with 95% efficiency," Opt. Express **16**, 3032–3040 (2008).
58. D. Fukuda, G. Fujii, T. Numata, K. Amemiya, A. Yoshizawa, H. Tsuchida, H. Fujino, H. Ishii, T. Itatani, S. Inoue, and T. Zama, "Titanium-based transition-edge photon number resolving detector with 98% detection efficiency with index-matched small-gap fiber coupling," Opt. Express **19**, 870–875 (2011).
59. T. Gerrits, A. Lita, B. Calkins, and S. W. Nam, "Superconducting transition edge sensors for quantum optics," in *Superconducting Devices in Quantum Optics* (Springer, 2016), pp. 31–60.
60. C. M. Natarajan, M. G. Tanner, and R. H. Hadfield, "Superconducting nanowire single-photon detectors: physics and applications," Supercond. Sci. Technol. **25**, 063001 (2012).
61. F. Marsili, V. B. Verma, J. A. Stern, S. Harrington, A. E. Lita, T. Gerrits, I. Vayshenker, B. Baek, M. D. Shaw, R. P. Mirin, and S. W. Nam, "Detecting single infrared photons with 93% system efficiency," Nat. Photonics **7**, 210–214 (2013).
62. C. Cahall, K. L. Nicolich, N. T. Islam, G. P. Lafyatis, A. J. Miller, D. J. Gauthier, and J. Kim, "Multi-photon detection using a conventional superconducting nanowire single-photon detector," Optica **4**, 1534–1535 (2017).
63. J. Tiffenberg, M. Sofo-Haro, A. Drlica-Wagner, R. Essig, Y. Guardincerri, S. Holland, T. Volansky, and T.-T. Yu, "Single-electron and single-photon sensitivity with a silicon skipper ccd," Phys. Rev. Lett. **119**, 131802 (2017).
64. M. M. Hayat, A. Joobeur, and B. E. Saleh, "Reduction of quantum noise in transmittance estimation using photon-correlated beams," J. Opt. Soc. Am. A **16**, 348–358 (1999).
65. A. Mood, F. Graybill, and D. Boes, *Introduction to the Theory of Statistics* (McGraw-Hill, 1974).
66. A. G. Frodesen, O. Skjeggestad, and H. Tofte, *Probability and Statistics in Particle Physics* (Universitetsforlagen, 1979).
67. D. V. Reddy, A. E. Lita, S. W. Nam, R. P. Mirin, and V. B. Verma, "Achieving 98% system efficiency at 1550 nm in superconducting nanowire single photon detectors," in *Rochester Conference on Coherence and Quantum Optics (CQO-11)* (Optical Society of America, 2019), paper W2B.2.
68. J.-L. Blanchet, F. Devaux, L. Furfaro, and E. Lantz, "Measurement of sub-shot-noise correlations of spatial fluctuations in the photon-counting regime," Phys. Rev. Lett. **101**, 233604 (2008).